Journal of Instrumentation

SISSA

PAPER • **OPEN ACCESS**

Data-driven precision determination of the material budget in ALICE

To cite this article: S. Acharya *et al* 2023 *JINST* **18** P11032

View the article online for updates and enhancements.

You may also like

- Search for Multimessenger Sources of Gravitational Waves and High-energy Neutrinos with Advanced LIGO during Its First Observing Run, ANTARES, and IceCube
A. Albert, M. André, M. Anghinolfi et al.
- Fast *b*-tagging at the high-level trigger of the ATLAS experiment in LHC Run 3
G. Aad, B. Abbott, K. Abeling et al.
- The ATLAS Fast TracKer system
The ATLAS collaboration, G. Aad, B. Abbott et al.



This content was downloaded from IP address 193.140.1.200 on 23/01/2024 at 11:19

Published by IOP Publishing for Sissa Medialab

Received: *April 7, 2023*
Accepted: *April 24, 2023*
Published: *November 30, 2023*

Data-driven precision determination of the material budget in ALICE



The ALICE collaboration

E-mail: ALICE-publications@cern.ch

Abstract: The knowledge of the material budget with a high precision is fundamental for measurements of direct photon production using the photon conversion method due to its direct impact on the total systematic uncertainty. Moreover, it influences many aspects of the charged-particle reconstruction performance. In this article, two procedures to determine data-driven corrections to the material-budget description in ALICE simulation software are developed. One is based on the precise knowledge of the gas composition in the Time Projection Chamber. The other is based on the robustness of the ratio between the produced number of photons and charged particles, to a large extent due to the approximate isospin symmetry in the number of produced neutral and charged pions. Both methods are applied to ALICE data allowing for a reduction of the overall material budget systematic uncertainty from 4.5% down to 2.5%. Using these methods, a locally correct material budget is also achieved. The two proposed methods are generic and can be applied to any experiment in a similar fashion.

Keywords: Analysis and statistical methods; Detector modelling and simulations I (interaction of radiation with matter, interaction of photons with matter, interaction of hadrons with matter, etc); Large detector systems for particle and astroparticle physics; Particle tracking detectors

ArXiv ePrint: 2303.15317

© 2023 CERN for the benefit of the ALICE collaboration. Published by IOP Publishing Ltd on behalf of Sissa Medialab. Original content from this work may be used under the terms of the Creative Commons Attribution 4.0 licence. Any further distribution of this work must maintain attribution to the author(s) and the title of the work, journal citation and DOI.

https://doi.org/10.1088/1748-0221/18/11/P11032

2023 JINST 18 P11032

Contents

1 Introduction 1

2 Detector description and data sample 2

3 Photon reconstruction 3

4 Calibration methods 5

4.1 TPC-gas based calibration weights: ω_i 6

4.2 Pion-isospin-symmetry based calibration weights: Ω_i 7

4.3 Comparison of the two calibration methods 8

5 Determination of ω_i and Ω_i 9

6 Conclusions 14

The ALICE collaboration 18

1 Introduction

The ALICE experiment is a dedicated heavy-ion experiment at the CERN LHC [1–3]. In ALICE, photons are measured using either the calorimeters (PHOS [4, 5], EMCal [6–8]), or the Photon Conversion Method (PCM) [2, 9], i.e. via the reconstruction of e^+e^- pairs from photon conversions in the detector material. The material budget is, expressed in % of radiation lengths, $X/X_0 = (11.4 \pm 0.5)\%$ [2, 9][1]. This value is an average over the pseudorapidity range $|\eta| < 0.9$ and it is integrated in the radial direction (R) up to 180 cm, where R is calculated in the transverse xy-plane to the beam axis (z). This uncertainty in the material budget translates into a systematic uncertainty of photon spectrum measurements. For example, direct-photon production[2] was measured in Pb–Pb collisions at a center of mass energy per nucleon pair of $\sqrt{s_{\rm NN}} = 2.76$ TeV in three centrality classes by ALICE [10]. The measurement was done by a combination of the independent PCM and PHOS measurements. A low transverse momentum ($p_{\rm T}$) excess with respect to perturbative Quantum Chromodynamics (pQCD) prompt-photon predictions is observed, which can be attributed to thermal photon emission from the quark–gluon plasma (QGP). The current uncertainties do not allow for discrimination among the proposed theoretical models [11–19]. For the events in the 0–20% centrality interval, the low $p_{\rm T}$ excess is of the order of 10–15%, and the total uncertainty is

[1] Obtained from the geometrical model of the ALICE experiment implemented in the simulation software.

[2] The terminology used for the different photon sources is as follows. Direct photons: all photons except from neutral meson decays. Thermal photons: photons from the QGP and hadron gas that are dominant at low transverse momentum ($p_{\rm T} < 3$ GeV/c). Prompt photons: produced in hard scatterings (calculable with pQCD) and pre-equlibrium photons that are dominant at high $p_{\rm T}$ ($p_{\rm T} > 5$ GeV/c).

2023 JINST 18 P11032

approximately 6% at low p_{T} with the largest contribution being the 4.5% of the material budget. Therefore, reducing the uncertainty of the material budget is essential for improving the significance of the direct-photon measurements and, thereby, allowing for a larger discrimination power among the different theoretical models.

The estimated systematic uncertainty related to the material budget of ±4.5% [2, 9] is an average over the R range given above. Initially, the systematic uncertainty was estimated by comparing the reconstructed number of γ conversions (N_γ) normalized to the number of charged particles (N_γ/N_{ch}) between real data (RD) and Monte Carlo (MC) simulations. Two event generators (PYTHIA 6 [20] and PHOJET 1.12 [21]), two secondary vertex finder algorithms with different optimization criteria, and two momentum ranges were considered. Local differences of up to 20% were observed in some parts of the detector. The development of new procedures to reduce the systematic uncertainty and to achieve a more accurate local description of the material budget in the simulation is therefore mandatory.

This article establishes two data-driven correction methods for a precise determination of the material budget of a given detector using reconstructed photon conversions. The methods are based either on the existence of a well-known piece of material (e.g. the TPC gas in the ALICE case) or on the robustness of the ratio N_γ/N_{ch} above a low p_{T} threshold which is largely due to the approximate isospin symmetry in pion production. The two methods are developed for the ALICE experiment but can, in principle, be employed in any other experiment.

This article is organized as follows. The ALICE experimental setup and event sample used in this article and the photon reconstruction are described in section 2, and section 3, respectively. The proposed correction procedures are introduced in section 4. The results are presented in section 5 followed by the conclusions in section 6.

2 Detector description and data sample

A comprehensive description of the ALICE experiment during the LHC Runs 1 and 2 and its performance can be found in refs. [1, 2]. The relevant detectors for this analysis are the Inner Tracking System (ITS) [22], the Time Projection Chamber (TPC) [23] and the V0 detectors [24] which are operated inside a magnetic field up to 0.5 T directed parallel to the beam axis. The ITS consists of six cylindrical layers of high resolution silicon tracking detectors. The two innermost layers located at a radial distance of 3.9 cm and 7.6 cm are silicon pixel detectors (SPD); the two intermediate layers are silicon drift detectors (SDD) positioned at 15.0 cm and at 23.9 cm; and the two outermost layers are silicon strip detectors (SSD) at 38.0 cm and 43.0 cm. It measures the position of the primary collision vertex, the impact parameter of the tracks, and improves considerably the track p_{T} resolution at high p_{T}. The SDD and SSD layers provide the amplitude of the charged signal that is used for particle identification through the measurement of the specific energy loss ($\mathrm{d}E/\mathrm{d}x$). The TPC is a large ($\sim 85\ \mathrm{m}^3$) cylindrical drift detector filled during 2017 with a $\mathrm{Ne/CO_2/N_2}$ (90/10/5) gas mixture. It covers a pseudorapidity acceptance of $|\eta| < 0.9$ over the full azimuthal range, with a maximum of 159 reconstructed space points along the path of the track. In addition to the space points for the track reconstruction, the TPC provides particle identification via the measurement of the $\mathrm{d}E/\mathrm{d}x$. The V0 detector, which is made of two arrays of 32 plastic scintillators located at $2.8 < \eta < 5.1$ (V0A) and $-3.7 < \eta < -1.7$ (V0C), is used for triggering on the collisions [24].

2023 JINST 18 P11032

The analyses presented here use the low intensity part (up to few hundred Hz interaction rate) of the data recorded in 2017 during the LHC pp run at $\sqrt{s}$ = 5.02 TeV. A total of about 4×10^7 pp collisions recorded with a minimum-bias (MB) trigger are used. The MB trigger was defined by signals in both V0 detectors in coincidence with a bunch crossing to minimize the contribution from diffractive interactions. Contamination from beam-induced background events, produced outside the interaction region, is removed using the timing information of the V0 detectors and taking into account the correlation between tracklets and clusters in the SPD detector [2]. The events used for the analysis are required to have a primary vertex in the fiducial region $|z| < 10\,\text{cm}$ along the beam-line direction. The primary vertex is reconstructed either using global tracks (with ITS and TPC information) or using SPD tracklets. The contamination from in-bunch pile-up events is removed offline by excluding events with multiple vertices reconstructed in the SPD [25].

In general, MC simulations use a geometrical model of the ALICE detectors, an event generator as input, and a particle transport software, GEANT3 [26] in the ALICE case.

3 Photon reconstruction

Photons are reconstructed by measuring the e^+e^- pairs produced in photon conversions in the detector material. Charged tracks are reconstructed in the ALICE central barrel with the ITS [22] and the TPC [23], working together or independently. Two secondary-vertex algorithms with different optimization criteria are used in this analysis to search for oppositely-charged track pairs originating from a common (secondary) vertex, referred to as V^0 [2]. The V^0 sample consists mainly of K^0_S, Λ, $\overline{\Lambda}$ decays and γ conversions. Selection criteria based on track quality, particle identification and the topology of a photon conversion are applied. The complete list of selection criteria is summarized in table 1. Electrons, positrons, and photons are required to be within $|\eta| < 0.8$. In order to ensure good track quality, a minimum track transverse momentum of 50 MeV/c and a fraction of TPC clusters over findable clusters (the number of geometrically possible clusters which can be assigned to a track) above 0.6 were required. The conversion point of the photon candidates should be inside the η acceptance and the conversion radius should be inside $0 < R < 180$ cm and within the limits given by the so called 'line cut' (see table 1) to ensure that the photons come from the primary vertex. Electron identification and pion rejection are performed by using the specific energy loss $\mathrm{d}E/\mathrm{d}x$ in the TPC. The selection and rejection criteria are based on the number of standard deviations ($n\sigma_e$ and $n\sigma_\pi$) around the electron and pion hypothesis, where σ is the standard deviation of the energy loss measurement. The remaining contamination from Λ, $\overline{\Lambda}$, and K^0_S is further reduced using a two-dimensional selection in the (α, q_T) distribution, known as the Armenteros-Podolanski plot [27]; α is the longitudinal momentum asymmetry of positive and negative daughter tracks, defined as $\alpha = (p^+_L - p^-_L)/(p^+_L + p^-_L)$, and q_T is the transverse momentum of the decay particles with respect to the V^0 momentum. Conversion electrons have a preferred emission orientation that can be described by the angle ψ_{pair} between the plane that is perpendicular to the magnetic field (x-y plane) and the plane defined by the opening angle of the pair. A selection on ψ_{pair} together with a cut on the photon χ^2 of the Kalman filter fit [28] further suppresses the contamination from non-photonic V^0 candidates. Monte Carlo simulations show that a photon purity above 99% is achieved at all transverse momenta except in the vicinity of $p_T \sim 0.3$ GeV/c where it decreases to 98%. Figure 1 shows the probability that a reconstructed electron

2023 JINST 18 P11032

Table 1. Selection criteria applied to the V^0 sample to select photons among the different particles.

Track reconstruction	
$e^{\pm}$ track p_T	$p_T > 0.05$ GeV/c
$e^{\pm}$ track η	$\lvert\eta\rvert < 0.8$
$N_{\text{clusters}}/N_{\text{findable clusters}}$	$> 60\%$
conversion radius	$0 < R < 180$ cm
line cut	$R > \lvert Z\rvert \times ZR_{\text{Slope}} - Z_0$ with $ZR_{\text{Slope}} = \tan(2 \times \arctan(\exp(-\eta_{\text{cut}})))$ where $Z_0 = 7$ cm, $\eta_{\text{cut}} = 0.8$
Track identification	
$n\sigma_e$ TPC	$-3 < n\sigma_e < 5$
$n\sigma_\pi$ TPC	$n\sigma_\pi > 2$ for $0.25 < p < 3.5$ GeV/c
	$n\sigma_\pi > 0.5$ for $p > 3.5$ GeV/c
Conversion γ topology	
q_T	$q_T < 0.05\sqrt{1-(\alpha/0.95)^2}$ GeV/c
photon fit quality	$\chi^2_{\text{max}} = 20$
ψ_{pair}	$\lvert\psi_{\text{pair}}\rvert < 0.1\,(1 - \chi^2/\chi^2_{\text{max}})$

carries a certain fraction of the photon energy ($x = p_e/p_\gamma$) for photon candidates below and above a momentum of 0.4 GeV/c. The RD as well as reconstructed distributions from a MC simulation based on PYTHIA 8 with the Monash 2013 tune [29, 30] as input event generator are shown. Converted photons with $p > 0.4$ GeV/c can be reconstructed with electron fractional energies from 0 to 1, while at lower p only largely symmetric conversions are detected. Differences between the data and MC distributions are largely due to different photon momentum distributions that are not yet equalized at this stage (see eq. (5.2)). A high purity in the photon sample can be inferred from the similarity of the red points (MC) and blue curves that represent only MC verified photons (figure 1).

Figure 2 displays the radial distribution of photon conversion vertices. The experimental data as well as reconstructed distributions from a MC simulation based on PYTHIA 8 with the Monash 2013 tune [29, 30] as input event generator are shown. The radial distribution of reconstructed conversion vertices clearly reveals the different detector structures corresponding to the ITS and TPC. The experimental distribution is compared to the one obtained from MC simulations that accounts for the time-dependent variations of the detector conditions. The main goal is to select the primary photon sample, i.e. photons coming from electromagnetic decays of neutral mesons or direct photons. Additionally, there are three types of background contributions shown in the figure that need special treatment. i) Primary e^+e^- pairs from π^0 (or η) Dalitz decays wrongly detected as conversion photons, mainly localized at radii smaller than 5 cm, can be suppressed by a minimum cut of 5 cm in the analysis. ii) Random combinatorial background, which is subtracted both in RD and MC based on the MC. iii) a 5–10% contribution of secondary photons [31] from weak decays of K^0_S (e.g. $K^0_S \rightarrow \pi^0\,\pi^0$) and Λ ($\overline{\Lambda}$) (e.g. $\Lambda \rightarrow n\pi^0$) hadrons, and interactions in the detector material. The contribution from weak decays is estimated in the data by using a particle decay simulation called "cocktail simulation" [32] based on parametrizations of measured particle spectra, and in MC using the full MC information (labelled 'True' in figure 2). The contribution from interactions

2023 JINST 18 P11032

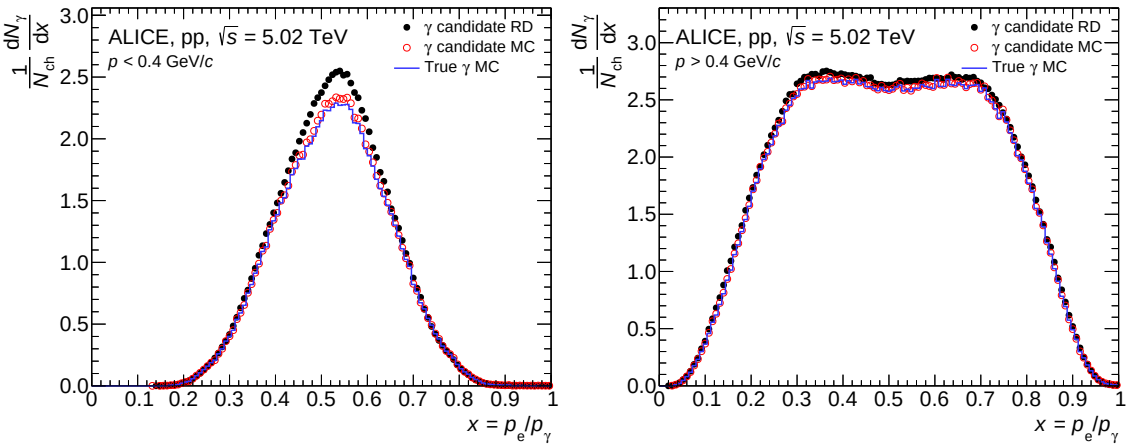


Figure 1. Distribution of the electron fractional energy (x) for photon candidates with $p < 0.4\,\mathrm{GeV}/c$ (left) and with $p > 0.4\,\mathrm{GeV}/c$ (right) reconstructed in real data (black points), in Monte Carlo simulations (red points), and for verified photons in MC simulations (blue lines) where PYTHIA8 is used as input event generator.

in the detector material is taken from MC, for both MC and real data (RD). The total secondary contribution is then subtracted from the photon sample in the data and in the MC simulated sample for each radial interval.

4 Calibration methods

The RD to MC comparison of the number of reconstructed photons as a function of the conversion point radius shown in figure 2 reveals local differences of up to 20% in the number of reconstructed photons[3]. This provides evidence that the implementation of the material budget in the geometrical model of ALICE is not accurate enough in some parts of the detector, which may impact the precision of various analyses in ALICE.

Two data-driven calibration methods (the ω_i and Ω_i calibration weights, section 4.1, section 4.2) were developed in order to mitigate the differences by correcting the detector material description in MC simulations, and thus, reducing the systematic uncertainty. The complete radial range is subdivided in twelve intervals as shown in figure 2. The resulting calibration weights are then used to scale the photon reconstruction efficiency as follows:

$$\epsilon_{\gamma}^{\mathrm{MC,corr}}(p_{\mathrm{T}}) = \frac{\sum_i W_i \times \mathrm{d}N_{\gamma,i}^{\mathrm{rec,MC}}/\mathrm{d}p_{\mathrm{T}}}{\mathrm{d}N_{\gamma}^{\mathrm{prod}}/\mathrm{d}p_{\mathrm{T}}}, \tag{4.1}$$

where W_{i} are the correction factors in each radial interval i ($W_i \equiv \omega_i$ or $W_i \equiv \Omega_i$), $\mathrm{d}N_{\gamma,i}^{\mathrm{rec,MC}}/\mathrm{d}p_{\mathrm{T}}$ is the number of primary photons reconstructed in the Monte Carlo simulated data at a given p_{T} and radial interval i (see figure 2) in the pseudorapidity range $|\eta| < 0.8$, and $\mathrm{d}N_{\gamma}^{\mathrm{prod}}/\mathrm{d}p_{\mathrm{T}}$ is the total number of photons produced at a given p_{T} as given by the input event generator used in the MC within the same pseudorapidity interval.

[3]This differences could not be reduced further by checks of the ALICE geometrical model

2023 JINST 18 P11032

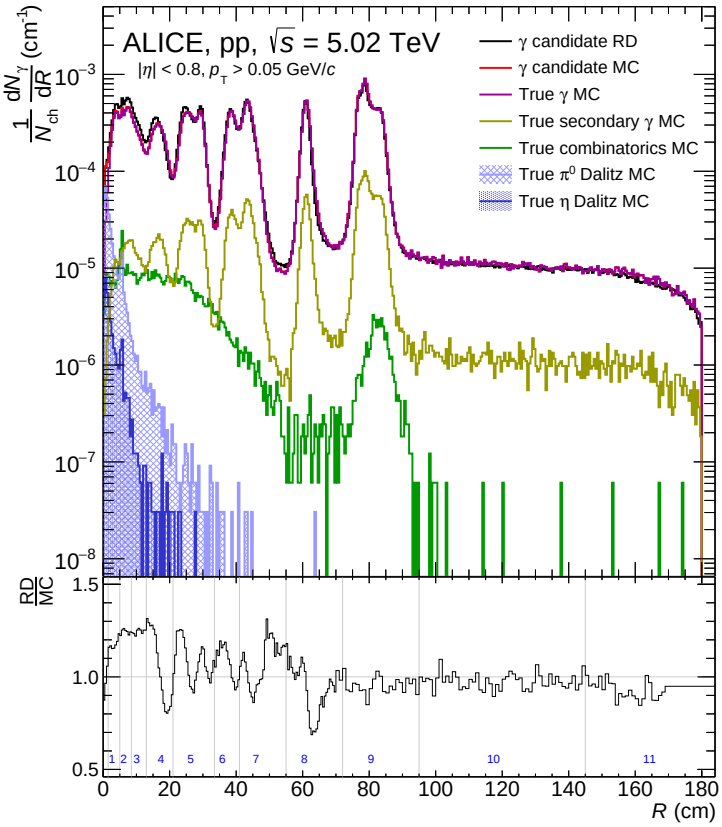


Figure 2. (Top) Radial distributions of reconstructed photon vertices in experimental data and in MC simulations are shown as black and red lines, respectively. Using the full MC information contributions from true photons (purple line), secondary photons (olive line), and combinatorial pairs (green line) are identified. The e^+e^- pairs from π^0 (or η) Dalitz decays, wrongly identified as photon conversions, are depicted as blue shaded areas. (Bottom) Ratio of the radial distribution of reconstructed photon vertices in RD (black line) and MC (red line). Vertical lines in grey and blue numbers indicate the twelve radial intervals and their respective indices used in the analysis.

Another approach for applying the calibration weights is to scale the density of the detector materials used in the geometrical model of the detector by the correction factors W_i, and produce new MC simulations. While the method given by eq. (4.1) is only valid for analyses involving photons, the scaling of the density is valid for all analyses. The only disadvantage is the need of creating new simulation samples, with the corresponding CPU needs.

4.1 TPC-gas based calibration weights: ω_i

The material-budget correction via ω_i calibration weights exploits the fact that a well-known and homogeneous part of the detector material can be used as a reference to calibrate the material budget of the rest of the detector known with less precision. The TPC gas volume [23] in the fiducial range used for photon reconstruction, $95 < R < 145$ cm, is perfectly suited for this purpose. The TPC gas material budget depends on the exact chemical composition, temperature and pressure of the gas. During data taking, variations in the TPC gas composition and pressure are monitored

2023 JINST 18 P11032

with a gas chromatograph and a pressure gauge, respectively, and applied accordingly in the MC simulations via access to the conditions and calibrations database with a granularity of few hours. The temperature gradients inside the TPC are controlled to a root-mean-square (rms) deviation of less than 0.05 °C [23] in order to control the drift properties. With the TPC gas monitoring system [23] the TPC gas density is known to the per mil level. The TPC-gas based calibration weights (ω_i) are then given by

$$\omega_i = \frac{N_{\gamma,i}^{\mathrm{rec,RD}} / N_{\gamma,\mathrm{gas}}^{\mathrm{rec,RD}}}{N'^{\mathrm{rec,MC}}_{\gamma,i} / N'^{\mathrm{rec,MC}}_{\gamma,\mathrm{gas}}}, \tag{4.2}$$

where $N_{\gamma,i}^{\mathrm{rec,X}}$ is the number of reconstructed primary photons in a given radial interval i (denoted by 'gas' for the reference one) expressed as

$$N_{\gamma,i}^{\mathrm{rec,X}} = \int_{p_{\mathrm{T,min}}}^{\infty} \tilde{P}_i^{\mathrm{X}}(p_{\mathrm{T}}) \times \tilde{\epsilon}_i^{\mathrm{X}}(p_{\mathrm{T}}) \frac{dN_{\gamma}^{\mathrm{prod,X}}}{dp_{\mathrm{T}}} dp_{\mathrm{T}} \equiv P_i^{\mathrm{X}} \times \epsilon_{\gamma,i}^{\mathrm{X}} \times N_{\gamma}^{\mathrm{prod,X}}, \tag{4.3}$$

where X refers both to RD and to MC, $p_{\mathrm{T,min}} = 0.05$ GeV/c, $N_{\gamma}^{\mathrm{prod}}$ is the number of produced primary photons either in RD or in MC. The photon conversion probability, and the photon reconstruction efficiency in a given radial interval i are denoted by P_i and $\epsilon_{\gamma,i}$, respectively. The reweighted $N'^{\mathrm{rec}}_{\gamma,i}$ is defined later in eq. (5.1). The photon reconstruction efficiency is calculated using MC simulations. The RD and MC labels are also used in the efficiency to emphasize possible differences of the RD efficiency compared to the values obtained in the MC simulations. The ratio between two radial intervals suppresses the impact of different numbers of produced photons, or the overall reconstruction efficiency, between data and Monte Carlo simulations.

4.2 Pion-isospin-symmetry based calibration weights: Ω_i

The material budget correction via the Ω_i calibration weights exploits the robustness of the ratio of the number of reconstructed photons to the number of reconstructed charged particles ($N_{\gamma}^{\mathrm{rec}} / N_{\mathrm{ch}}^{\mathrm{rec}}$) above a certain low p_{T} threshold. The reason for the robustness is the approximate isospin symmetry [33] in the number of produced charged and neutral pions, and that charged pions and photons from π^0 decays are the dominant contributions to the number of charged particles (90% of charged particles are charged pions) [34, 35] and the total number of photons [32], respectively. 'Approximate' is used to point out that electromagnetic decays of the η, ω and η' mesons are cases that violate the pion isospin symmetry. By employing PYTHIA 8 and PHOJET [21] event generators it was checked that the ratio is constant at the per mil level even if the charged-particle multiplicity or the photon multiplicity differ by 10–20% depending on the collision energy and event generator. In summary, the ratio of the number of reconstructed primary photons in a given radial interval ($N_{\gamma,i}^{\mathrm{rec}}$) divided by the number of reconstructed primary charged particles (N_{ch}) in RD over the same quantity in MC (Ω_i) is sensitive to the correctness of the detector material implementation; thus, the Ω_i can be used as calibration weights.

The pion-isospin-symmetry based calibration weights (Ω_i) are then defined as

$$\Omega_i = \frac{N_{\gamma,i}^{\mathrm{rec,RD}} / N_{\mathrm{ch}}^{\mathrm{rec,RD}}}{N'^{\mathrm{,rec,MC}}_{\gamma,i} / N_{\mathrm{ch}}^{\mathrm{rec,MC}}}, \tag{4.4}$$

2023 JINST 18 P11032

where ($N_{\rm ch}^{\rm rec,X}$) is the number of reconstructed primary tracks with a transverse momentum $p_{\rm T} > 0.15$ GeV/c in the pseudorapidity range $|\eta| < 0.8$, X refers to RD or to MC, and $N_{\gamma,i}^{\rm rec}$ is the number of reconstructed primary photons in the radial interval i with transverse momentum above a minimum value of 0.05 GeV/c (see eq. (4.3)). The reweighted $N'^{\rm rec}_{\gamma,i}$ is defined later in eq. (5.1). Charged tracks are selected with selections on the number of space points used for tracking and on the quality of the track fit, as well as on the distance of closest approach to the reconstructed vertex [35]. The contribution of secondary charged particles is subtracted in the case of data using the measurement performed in ALICE in the same data set [35], and in MC using the full MC information. The normalization to $N_{\rm ch}$ minimizes the impact of the model dependence of a given inclusive photon production yield $N_{\gamma}^{\rm prod}$ in an event generator relative to RD.

4.3 Comparison of the two calibration methods

The comparison of the two calibration factors described in section 4.1 and section 4.2 carries very valuable information. In order to gain insights into potential differences between the two sets of correction factors, it is useful to write them in terms of the conversion probability P_i in a given radial interval.

Taking into account eq. (4.3), the ω_i calculation given by eq. (4.2) transforms into

$$\omega_i = \frac{P_i^{\rm RD} \times \epsilon_{\gamma,i}^{\rm RD}}{P_i^{\rm MC} \times \epsilon_{\gamma,i}^{\rm MC}} \times \frac{P_{\rm gas}^{\rm MC} \times \epsilon_{\gamma,\rm gas}^{\rm MC}}{P_{\rm gas}^{\rm RD} \times \epsilon_{\gamma,\rm gas}^{\rm RD}}. \tag{4.5}$$

Under the assumption that the gas is a well-known material, the conversion probabilities in MC and RD agree for the reference radial interval, i.e.

$$P_{\rm gas}^{\rm RD} = P_{\rm gas}^{\rm MC}. \tag{4.6}$$

Then, the ω_i calculation given by eq. (4.5) reduces to

$$\omega_i = \frac{P_i^{\rm RD} \times \epsilon_{\gamma,i}^{\rm RD} \times \epsilon_{\gamma,\rm gas}^{\rm MC}}{P_i^{\rm MC} \times \epsilon_{\gamma,i}^{\rm MC} \times \epsilon_{\gamma,\rm gas}^{\rm RD}}, \tag{4.7}$$

For the pion-isospin-symmetry based calibration method, Ω_i, the number of reconstructed primary charged particles ($N_{\rm ch}$) in the same $|\eta|$ range is also needed:

$$N_{\rm ch}^{\rm rec,X} = N_{\rm ch}^{\rm prod,X} \times \epsilon_{\rm track}^{\rm X}, \tag{4.8}$$

where X refers to RD or MC.

Using eq. (4.4) and eq. (4.8) the Ω_i are given by

$$\Omega_i = \frac{P_i^{\rm RD} \times \epsilon_{\gamma,i}^{\rm RD} \times \epsilon_{\rm track}^{\rm MC} \times N_{\gamma}^{\rm prod,RD}/N_{\rm ch}^{\rm prod,RD}}{P_i^{\rm MC} \times \epsilon_{\gamma,i}^{\rm MC} \times \epsilon_{\rm track}^{\rm RD} \times N_{\gamma}^{\rm prod,MC}/N_{\rm ch}^{\rm prod,MC}}. \tag{4.9}$$

By employing the same MC simulations with PYTHIA 8 and PHOJET as event generators it was verified that the quantity $N_{\gamma}^{\rm prod}/N_{\rm ch}^{\rm prod}$ is constant within approximately 1.5% when varying $p_{\rm T,min}$ between 0.15 GeV/c and 0.25 GeV/c. The $p_{\rm T,min}$ value reduces the diffractive contribution that is different among the two event generators. In this work, the value for the ratio $N_{\gamma}^{\rm prod}/N_{\rm ch}^{\rm prod}$ obtained

2023 JINST 18 P11032

from PYTHIA is assumed for RD and differences between PYTHIA and PHOJET are taken as part of the systematic uncertainties. With this assumption for the quantity $N_\gamma^{\rm prod}/N_{\rm ch}^{\rm prod}$, the calibration weights Ω_i reduce to

$$\Omega_i = \frac{P_i^{\rm RD} \times \epsilon_{\gamma,i}^{\rm RD} \times \epsilon_{\rm track}^{\rm MC}}{P_i^{\rm MC} \times \epsilon_{\gamma,i}^{\rm MC} \times \epsilon_{\rm track}^{\rm RD}}. \tag{4.10}$$

In case a constant ($p_{\rm T}$ and R-independent) factor between the V^0 reconstruction efficiencies in RD and MC would exist ($\epsilon_{\gamma,i}^{\rm RD}/\epsilon_{\gamma,i}^{\rm MC}$) it would drop out for the ω_i weights (see eq. (4.5)). According to eq. (4.10) this is not the case for Ω_i weights.

Using eq. (4.5) or eq. (4.7) and eq. (4.10), the ratio Ω_i/ω_i is given by

$$\frac{\Omega_i}{\omega_i} = \frac{P_{\rm gas}^{\rm RD} \times \epsilon_{\gamma,\rm gas}^{\rm RD} \times \epsilon_{\rm track}^{\rm MC}}{P_{\rm gas}^{\rm MC} \times \epsilon_{\gamma,\rm gas}^{\rm MC} \times \epsilon_{\rm track}^{\rm RD}}, \tag{4.11}$$

or

$$\frac{\Omega_i}{\omega_i} = \frac{\epsilon_{\gamma,\rm gas}^{\rm RD} \times \epsilon_{\rm track}^{\rm MC}}{\epsilon_{\gamma,\rm gas}^{\rm MC} \times \epsilon_{\rm track}^{\rm RD}}. \tag{4.12}$$

By calculating the Ω_i/ω_i ratio one can cross-check if the ratio $\epsilon_{\gamma,\rm gas}/\epsilon_{\rm track}$, i.e. the reconstruction efficiency in the reference radial interval 'gas' over the charged particle reconstruction efficiency, is reproduced in MC. In case $\Omega_i/\omega_i \neq 1$, the ω_i calibration weights cannot be used directly as correction factors.

5 Determination of ω_i and Ω_i

All quantities that are needed to compute the ω_i and Ω_i correction factors are introduced in section 4. The calculation of the ω_i and Ω_i weights follows an iterative procedure because, as the photon reconstruction efficiency is different for the various radial intervals, the differences between the reconstructed number of photons in RD and in MC can also result from a deviation of the shape of the MC photon $p_{\rm T}$ spectrum from RD. In order to take this effect into account, the shape of the MC simulated photon transverse momentum spectrum is adjusted to the measured shape in RD by applying weights ($\Theta(p_{\rm T})$) to the MC simulated data as

$$\mathrm{d}N'^{\rm rec,MC}_{\gamma}/\mathrm{d}p_{\rm T} = \mathrm{d}N_\gamma^{\rm rec,MC}/\mathrm{d}p_{\rm T} \times \Theta(p_{\rm T}), \tag{5.1}$$

where $\Theta(p_{\rm T})$ is defined as

$$\Theta(p_{\rm T}) = \frac{N_\gamma^{\rm rec,MC}}{N_\gamma^{\rm rec,RD}} \times \frac{\mathrm{d}N_\gamma^{\rm rec,RD}/\mathrm{d}p_{\rm T}}{\mathrm{d}N_\gamma^{\rm rec,MC}/\mathrm{d}p_{\rm T}}. \tag{5.2}$$

The total number of photons is preserved as only the shape of the spectrum is modified,

$$N'^{\rm rec,MC}_{\gamma} = N_\gamma^{\rm rec,MC}. \tag{5.3}$$

The first step is to align the shape of the reconstructed transverse momentum distributions of the MC to the data (eq. (5.1)) using the $\Theta(p_{\rm T})$ factors given in eq. (5.2). This step is performed twice to achieve good agreement. A set of ω_i and Ω_i is then obtained using eq. (4.2) and eq. (4.4), respectively. Applying the Ω_i calibration weights results in a modification of the reconstructed transverse momentum distribution. Therefore, a second iteration of the complete procedure is

2023 JINST 18 P11032

Table 2. Sources of the relative systematic uncertainties (%) of Ω_i and ω_i for two radial intervals. The V^0 finder category includes uncertainties on the reconstruction efficiency and its p_T and R dependence, track selection criteria, as well as two V^0 finder methods. The generator category includes uncertainties on the robustness of N_γ/N_{ch}. The total systematic uncertainty is given in the last row.

	Ω_i		ω_i	
	5 cm < R < 8.5 cm	95 cm < R < 145 cm	8.5 cm < R < 13 cm	72 cm < R < 95 cm
V^0 finder	2.74 %	2.9%	2.2%	1.83%
Generator	0.16%	2.9%	3.2 %	0.62 %
$p_{T,min}$	Negligible	Negligible	Negligible	Negligible
σ_{sys}	2.74%	4.1%	3.8%	1.93%

performed, i.e. a new set of $\Theta(p_T)$ and Ω_i is computed. Applying this new set of Ω_i does not introduce any further change in the transverse momentum distribution, i.e. the procedure of evaluating ω_i and Ω_i weights converged.

Four combinations of input event generators and V^0 finders are tested and used for the evaluation of the systematic uncertainties. PYTHIA 8 with the Monash 2013 tune [29, 30] and PHOJET 1.12 [21], available within the DPMJET 3.0 [36] package, are used. The default combination is using PYTHIA 8 as event generator, since the Monash tune is the result of an optimization for the LHC data. For PHOJET larger differences as compared with PYTHIA 8 are observed in the simulated charged-particle multiplicity distributions compared to experimental data. Both event generators show differences in the transverse momentum spectrum with respect to experimental data. These differences are considered as part of the systematic uncertainties of the resulting material budget weights. The two V^0 finders are called "on-the-fly" and "offline". The "on-the-fly" V^0 finder searches for V^0 candidates during the tracking procedure, when the complete detector information, down to reconstructed clusters is available. The "offline" V^0 finder searches for V^0 candidates based on reconstructed tracks, which includes their full momentum vector and uncertainty covariance matrix, but no cluster level information. Each method results in a somewhat different performance in terms of reconstruction efficiency at different radii. The "on-the-fly" V^0 finder is the default choice for the calculation of the Ω_i and ω_i calibration weights, mostly because of its significantly larger efficiency, and because the photon momenta are calculated at the conversion point. By varying the V^0 finder, uncertainties on the reconstruction efficiency and its p_T and R dependence, track selection criteria, and the secondary-vertex algorithm in itself are included. By varying the event generator, uncertainties on the robustness of N_γ/N_{ch} are included. An additional variation of $p_{T,min}$ from 0.05 GeV/c up to 0.2 GeV/c does not yield a sizeable difference in either of the methods.

The systematic uncertainties of the weights Ω_i are calculated according to

$$\sigma_{V^0\,\text{finder}} = |W_i^{\text{PYTHIA,on-the-fly}} - W_i^{\text{PYTHIA,offline}}|, \tag{5.4}$$

$$\sigma_{\text{generator}} = |W_i^{\text{PYTHIA,on-the-fly}} - W_i^{\text{PHOJET,on-the-fly}}|, \tag{5.5}$$

$$\sigma^2_{\text{sys}}(W_i) = \sigma^2_{V^0\,\text{finder}}(W_i) + \sigma^2_{\text{generator}}(W_i), \tag{5.6}$$

where $W_i \equiv \omega_i$ or $W_i \equiv \Omega_i$. Table 2 shows details for two selected radial intervals.

2023 JINST 18 P11032

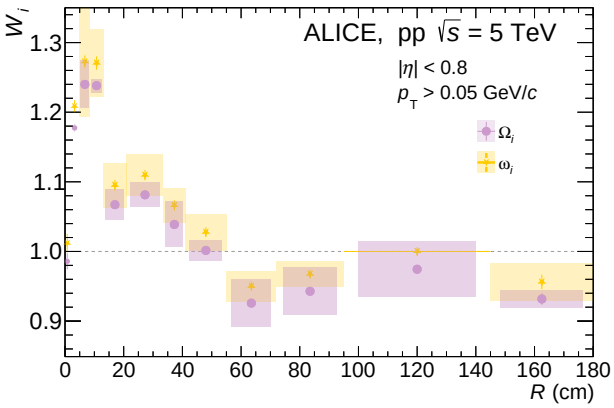


Figure 3. Distribution of the weights Ω_i and ω_i as a function of the radial position of the conversion point. Statistical uncertainties are given by the vertical bars, and systematic uncertainties are depicted by shaded areas, except for the first two intervals where only statistical uncertainties are quoted. Notice the zero ω_i systematic uncertainty in the calibration intervals (95 cm< R < 145 cm), thus an horizontal line is drawn displaying the radial interval. The width in spatial direction of the uncertainty box for the Ω_i was shrunk for better visibility.

The radially averaged weight $\langle\Omega\rangle$ is given by

$$\langle\Omega\rangle = \sum_i \frac{N_\gamma^{\mathrm{i}}}{N_\gamma^{\mathrm{total}}} \times \Omega_i, \tag{5.7}$$

and, assuming that the statistical uncertainties are negligible and the systematic uncertainties are correlated among the different radial intervals, its uncertainty $\sigma(\Omega)$ is given by

$$\sigma(\Omega) = \sum_i \frac{N_\gamma^{\mathrm{i}}}{N_\gamma^{\mathrm{total}}} \times \sigma(\Omega_i). \tag{5.8}$$

The final set of ω_i and Ω_i calibration weights is presented in figure 3. The calibration weights range from a minimum value of 0.926 ± 0.034 to a maximum of 1.240 ± 0.034, corresponding to the TPC inner containment vessel (interval 8) and the silicon pixels plus thermal shield (interval 2), respectively. The two sets of calibration weights, Ω_i and ω_i, are very similar to each other, differing by only about 2.5%. On the other hand, one observes that for R < 55 cm the uncertainties of Ω_i are smaller than for ω_i, while they are larger for R > 55 cm. The reason is that in the case of ω_i the uncertainties in the gas add to the corresponding ones in the given interval for R < 55 cm because the mean momentum of the reconstructed photons in radial intervals "gas" and "i" are different, while, as the radial interval comes closer to the one in the gas (R > 55 cm), part of the uncertainties cancels out. According to eq. (4.12), a difference in the ratio can be attributed to small differences in the reconstruction efficiency ratio ($\epsilon_{\gamma,\mathrm{gas}}/\epsilon_{\mathrm{track}}$) in RD with respect to the one obtained in the MC simulations, or even differences in the reference calibration material (P_{gas}, see eq. (4.11)). As a small difference of 2.5% is observed, the ω_i correction factors cannot be taken directly as material budget correction (see section 4.3 and eq. (4.12)). Consequently, the values of Ω_i as shown in figure 3 and given in table 3 are taken as the best correction factors.

2023 JINST 18 P11032

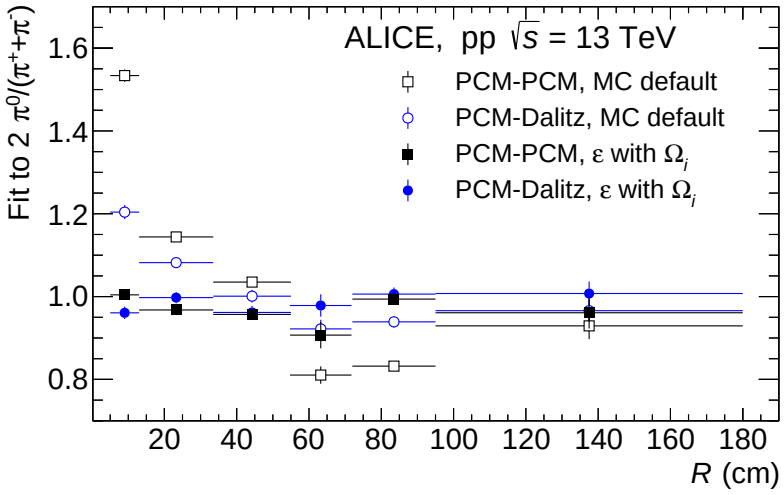


Figure 4. Zero-order polynomial fits to the ratio of neutral to charged pion transverse momentum distributions above 1 GeV/c when the two photons (PCM-PCM, $\pi^0 \rightarrow \gamma\gamma$) or one photon (PCM-Dalitz, $\pi^0 \rightarrow e^+e^-\gamma$) are selected within the given radial interval. The open symbols are obtained with efficiency corrections using the default MC , while the full symbols are obtained when the Ω_i calibration factors are used to weight the efficiency (see eq. (4.1)).

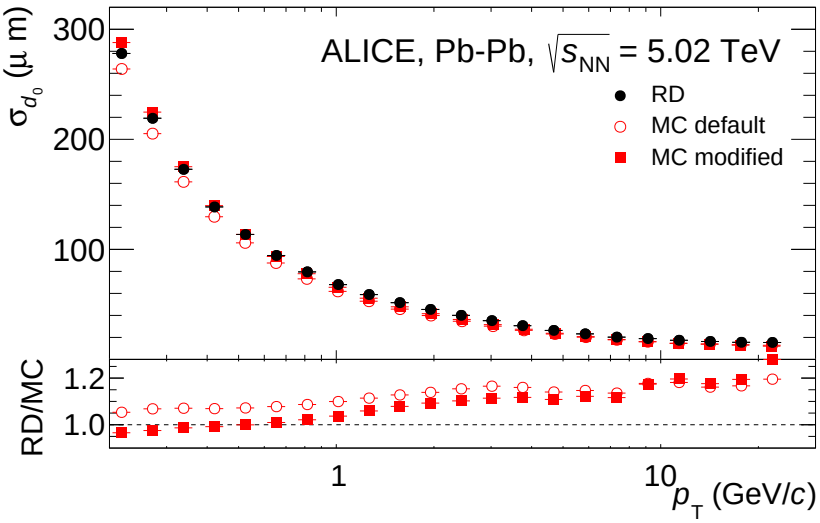


Figure 5. Top: Impact-parameter resolution of reconstructed charged particles requiring a hit in the first ITS pixel layer as a function of p_T in RD, default MC, and modified MC with the correction factors as given in table 3. Bottom: Ratio of impact-parameter resolution to the one in the default MC (open circles) and modified MC (squares).

2023 JINST 18 P11032

Table 3. Correction factors Ω_i for each radial interval used in this analysis, as well as the average value. Statistical, systematic, and total uncertainties are also given, except for the first two intervals where only statistical uncertainties are quoted.

R interval	R range (cm)	Ω_i	σ_{stat} %	σ_{sys} %	σ_{total} %
0	0–1.5	0.9859	1.2	—	—
1	1.5–5	1.177	0.42	—	—
2	5–8.5	1.240	0.36	2.7	2.8
3	8.5–13	1.238	0.42	0.77	0.9
4	13–21	1.067	0.34	2.0	2.1
5	21–33.5	1.081	0.25	1.7	1.7
6	33.5–41	1.039	0.35	3.1	3.1
7	41–55	1.001	0.30	1.5	1.5
8	55–72	0.926	0.35	3.7	3.7
9	72–95	0.943	0.19	3.7	3.7
10	95–145	0.975	0.62	4.1	4.1
11	145–180	0.932	0.89	1.4	1.6
average	5–180	1.04	0.312%	2.5%	2.5%

In order to further verify the correctness of the Ω_i values, π^0 measurements [9, 37–39] are carried out selecting photons in a given radial interval at a time, before and after applying the correction factors. The transverse momentum spectra of π^0 should not depend on the radial interval where the photons are reconstructed. π^0 transverse momentum spectra measured with two (or one) decay photons within one radial interval[4] were analysed and compared to the spectra of charged pions [40], by fitting their ratios with a constant (see figure 4). The dispersion (rms) of the fit results is large when using the default MC. The fit results show clearly the same pattern as the calibration weights for the PCM-Dalitz analysis while for the PCM-PCM analysis the expected quadratic effect is observed. When using the Ω_i, the rms reduces by almost a factor 10 when both photons are reconstructed with the PCM method, or by a factor ~ 4 when only one PCM photon is used in the reconstruction, i.e., reconstructing either the Dalitz decay or reconstructing the second photon with a calorimeter. Furthermore, the ratio of the π^0 measurement in the complete radial range to the charged-pion measurement is in good agreement with the PYTHIA 8 expectations within one standard deviation.

Another observation corroborating the need for material budget correction factors is that the impact-parameter resolution of charged particles, i.e., the resolution of the reconstructed distance of closest approach of a track to the primary vertex, in RD is underestimated by the default MC. The small difference between data and MC of the particle composition plays a negligible effect, as most of the charged particles are charged pions. Figure 5 shows the impact-parameter resolution of reconstructed charged particles with a hit in the first ITS pixel layer as a function of p_{T} for RD and for the default MC. The difference between RD and MC is usually corrected with an ad-hoc smearing of the track parameters in the MC. On the other hand, a modified MC simulation where the correction factors as given in table 3 are used to scale the density of the detector materials

[4]For the Dalitz or the hybrid (PCM-EMC or PCM-PHOS) reconstruction methods, the selection of the radial interval only applies to the PCM photon.

2023 JINST 18 P11032

reproduces the measured resolution for $p_{\mathrm{T}} < 1$ GeV/c, where the multiple scattering contribution is largest. This result confirms also that the assumption of attributing the correction factors to the material budget and not to the efficiency is correct. This demonstrates the importance of the material budget correction well beyond the reconstruction of photons with the conversion method.

6 Conclusions

Two data-driven calibration methods of the detector material description in ALICE, one based on the precise knowledge of the ALICE TPC gas and the other based on the approximate pion isospin symmetry and named ω_i and Ω_i, were developed. A reduction of the systematic uncertainty of almost a factor of two is achieved in the material budget up to a radius $R = 180$ cm corresponding approximately to the radial center of the TPC. Moreover, the differences between the description of the material distribution used for MC and the reality in the individual R intervals are mitigated. This addresses the largest source of systematic uncertainty in analyses using photon conversions. It also reduces an important, and sometimes dominant, source of systematic uncertainty in analyses based on charged-particle tracking, in particular when secondary vertices are used. The upgraded ALICE experiment for Run 3 [41] will continue to use these two calibration methods. Moreover, to assist the ω_i method, two calibrated tungsten wires were inserted in the inner and the outer barrels of ITS2 [42]. These two methods are general in nature and could be applied to any experiment in a similar fashion.

Acknowledgments

The ALICE Collaboration would like to thank all its engineers and technicians for their invaluable contributions to the construction of the experiment and the CERN accelerator teams for the outstanding performance of the LHC complex. The ALICE Collaboration gratefully acknowledges the resources and support provided by all Grid centres and the Worldwide LHC Computing Grid (WLCG) collaboration. The ALICE Collaboration acknowledges the following funding agencies for their support in building and running the ALICE detector: A. I. Alikhanyan National Science Laboratory (Yerevan Physics Institute) Foundation (ANSL), State Committee of Science and World Federation of Scientists (WFS), Armenia; Austrian Academy of Sciences, Austrian Science Fund (FWF): [M 2467-N36] and Nationalstiftung für Forschung, Technologie und Entwicklung, Austria; Ministry of Communications and High Technologies, National Nuclear Research Center, Azerbaijan; Conselho Nacional de Desenvolvimento Científico e Tecnológico (CNPq), Financiadora de Estudos e Projetos (Finep), Fundação de Amparo à Pesquisa do Estado de São Paulo (FAPESP) and Universidade Federal do Rio Grande do Sul (UFRGS), Brazil; Bulgarian Ministry of Education and Science, within the National Roadmap for Research Infrastructures 2020¿2027 (object CERN), Bulgaria; Ministry of Education of China (MOEC), Ministry of Science & Technology of China (MSTC) and National Natural Science Foundation of China (NSFC), China; Ministry of Science and Education and Croatian Science Foundation, Croatia; Centro de Aplicaciones Tecnológicas y Desarrollo Nuclear (CEADEN), Cubaenergía, Cuba; Ministry of Education, Youth and Sports of the Czech Republic, Czech Republic; The Danish Council for Independent Research | Natural Sciences, the VILLUM FONDEN and Danish National Research Foundation (DNRF), Denmark;

2023 JINST 18 P11032

Helsinki Institute of Physics (HIP), Finland; Commissariat à l'Energie Atomique (CEA) and Institut National de Physique Nucléaire et de Physique des Particules (IN2P3) and Centre National de la Recherche Scientifique (CNRS), France; Bundesministerium für Bildung und Forschung (BMBF) and GSI Helmholtzzentrum für Schwerionenforschung GmbH, Germany; General Secretariat for Research and Technology, Ministry of Education, Research and Religions, Greece; National Research, Development and Innovation Office, Hungary; Department of Atomic Energy Government of India (DAE), Department of Science and Technology, Government of India (DST), University Grants Commission, Government of India (UGC) and Council of Scientific and Industrial Research (CSIR), India; National Research and Innovation Agency - BRIN, Indonesia; Istituto Nazionale di Fisica Nucleare (INFN), Italy; Japanese Ministry of Education, Culture, Sports, Science and Technology (MEXT) and Japan Society for the Promotion of Science (JSPS) KAKENHI, Japan; Consejo Nacional de Ciencia (CONACYT) y Tecnología, through Fondo de Cooperación Internacional en Ciencia y Tecnología (FONCICYT) and Dirección General de Asuntos del Personal Academico (DGAPA), Mexico; Nederlandse Organisatie voor Wetenschappelijk Onderzoek (NWO), Netherlands; The Research Council of Norway, Norway; Commission on Science and Technology for Sustainable Development in the South (COMSATS), Pakistan; Pontificia Universidad Católica del Perú, Peru; Ministry of Education and Science, National Science Centre and WUT ID-UB, Poland; Korea Institute of Science and Technology Information and National Research Foundation of Korea (NRF), Republic of Korea; Ministry of Education and Scientific Research, Institute of Atomic Physics, Ministry of Research and Innovation and Institute of Atomic Physics and University Politehnica of Bucharest, Romania; Ministry of Education, Science, Research and Sport of the Slovak Republic, Slovakia; National Research Foundation of South Africa, South Africa; Swedish Research Council (VR) and Knut & Alice Wallenberg Foundation (KAW), Sweden; European Organization for Nuclear Research, Switzerland; Suranaree University of Technology (SUT), National Science and Technology Development Agency (NSTDA), Thailand Science Research and Innovation (TSRI) and National Science, Research and Innovation Fund (NSRF), Thailand; Turkish Energy, Nuclear and Mineral Research Agency (TENMAK), Turkey; National Academy of Sciences of Ukraine, Ukraine; Science and Technology Facilities Council (STFC), United Kingdom; National Science Foundation of the United States of America (NSF) and United States Department of Energy, Office of Nuclear Physics (DOE NP), United States of America. In addition, individual groups or members have received support from: European Research Council, Strong 2020 - Horizon 2020 (grant nos. 950692, 824093), European Union; Academy of Finland (Center of Excellence in Quark Matter) (grant nos. 346327, 346328), Finland; Programa de Apoyos para la Superación del Personal Académico, UNAM, Mexico.

References

[1] ALICE collaboration, *The ALICE experiment at the CERN LHC*, 2008 *JINST* **3** S08002 [INSPIRE].

[2] ALICE collaboration, *Performance of the ALICE experiment at the CERN LHC*, *Int. J. Mod. Phys. A* **29** (2014) 1430044 [arXiv:1402.4476] [INSPIRE].

[3] ALICE collaboration, *The ALICE experiment — A journey through QCD*, arXiv:2211.04384 [INSPIRE].

[4] ALICE collaboration, *ALICE Photon Spectrometer (PHOS): technical design report*, CERN-LHCC-99-004, CERN, Geneva (1999).

[5] ALICE collaboration, *Calibration of the photon spectrometer PHOS of the ALICE experiment*, 2019 *JINST* **14** P05025 [arXiv:1902.06145] [INSPIRE].

[6] ALICE collaboration, *ALICE Electromagnetic Calorimeter Technical Design Report*, CERN-LHCC-2008-014 (2008).

[7] J. Allen et al., *ALICE DCal: an addendum to the EMCal technical design report di-jet and hadron-Jet correlation measurements in ALICE*, CERN-LHCC-2010-011 (2010).

[8] ALICE collaboration, *Performance of the ALICE Electromagnetic Calorimeter*, arXiv:2209.04216 [INSPIRE].

[9] ALICE collaboration, *Neutral pion and η meson production in proton-proton collisions at $\sqrt{s} = 0.9$ TeV and $\sqrt{s} = 7$ TeV*, *Phys. Lett. B* **717** (2012) 162 [arXiv:1205.5724] [INSPIRE].

[10] ALICE collaboration, *Direct photon production in Pb-Pb collisions at $\sqrt{s_{NN}} = 2.76$ TeV*, *Phys. Lett. B* **754** (2016) 235 [arXiv:1509.07324] [INSPIRE].

[11] H. van Hees, M. He and R. Rapp, *Pseudo-critical enhancement of thermal photons in relativistic heavy-ion collisions?*, *Nucl. Phys. A* **933** (2015) 256 [arXiv:1404.2846] [INSPIRE].

[12] J.-F. Paquet et al., *Production of photons in relativistic heavy-ion collisions*, *Phys. Rev. C* **93** (2016) 044906 [arXiv:1509.06738] [INSPIRE].

[13] R. Chatterjee, H. Holopainen, T. Renk and K.J. Eskola, *Collision centrality and τ_0 dependence of the emission of thermal photons from fluctuating initial state in ideal hydrodynamic calculation*, *Phys. Rev. C* **85** (2012) 064910 [arXiv:1204.2249] [INSPIRE].

[14] R. Chatterjee, L. Bhattacharya and D.K. Srivastava, *Electromagnetic probes*, *Lect. Notes Phys.* **785** (2010) 219 [arXiv:0901.3610] [INSPIRE].

[15] O. Linnyk et al., *Hadronic and partonic sources of direct photons in relativistic heavy-ion collisions*, *Phys. Rev. C* **92** (2015) 054914 [arXiv:1504.05699] [INSPIRE].

[16] M. He, R.J. Fries and R. Rapp, *Ideal hydrodynamics for bulk and multistrange hadrons in $\sqrt{s_{NN}} = 200$ AGeV Au-Au collisions*, *Phys. Rev. C* **85** (2012) 044911 [arXiv:1112.5894] [INSPIRE].

[17] N.P.M. Holt, P.M. Hohler and R. Rapp, *Thermal photon emission from the $\pi\rho\omega$ system*, *Nucl. Phys. A* **945** (2016) 1 [arXiv:1506.09205] [INSPIRE].

[18] M. Heffernan, P. Hohler and R. Rapp, *Universal parametrization of thermal photon rates in hadronic matter*, *Phys. Rev. C* **91** (2015) 027902 [arXiv:1411.7012] [INSPIRE].

[19] S. Turbide, R. Rapp and C. Gale, *Hadronic production of thermal photons*, *Phys. Rev. C* **69** (2004) 014903 [hep-ph/0308085] [INSPIRE].

[20] T. Sjostrand, S. Mrenna and P.Z. Skands, *PYTHIA 6.4 physics and Manual*, *JHEP* **05** (2006) 026 [hep-ph/0603175] [INSPIRE].

[21] R. Engel, J. Ranft and S. Roesler, *Hard diffraction in hadron hadron interactions and in photoproduction*, *Phys. Rev. D* **52** (1995) 1459 [hep-ph/9502319] [INSPIRE].

[22] ALICE collaboration, *Alignment of the ALICE Inner Tracking System with cosmic-ray tracks*, 2010 *JINST* **5** P03003 [arXiv:1001.0502] [INSPIRE].

[23] J. Alme et al., *The ALICE TPC, a large 3-dimensional tracking device with fast readout for ultra-high multiplicity events*, *Nucl. Instrum. Meth. A* **622** (2010) 316 [arXiv:1001.1950] [INSPIRE].

2023 JINST 18 P11032

[24] ALICE collaboration, *Performance of the ALICE VZERO system*, 2013 *JINST* **8** P10016 [arXiv:1306.3130] [INSPIRE].

[25] ALICE collaboration, *Charged-particle multiplicities in proton–proton collisions at* $\sqrt{s}$ = 0.9 *to 8 TeV*, *Eur. Phys. J. C* **77** (2017) 33 [arXiv:1509.07541] [INSPIRE].

[26] R. Brun et al., *GEANT3*, CERN-DD-EE-84-1 (1987) [INSPIRE].

[27] J. Podolanski and R. Armenteros, *III. Analysis of V-events*, *Phil. Mag.* **45** (1954) 13.

[28] I. Kisel, I. Kulakov and M. Zyzak, *Standalone first level event selection package for the CBM experiment*, *IEEE Trans. Nucl. Sci.* **60** (2013) 3703.

[29] T. Sjöstrand et al., *An introduction to PYTHIA 8.2*, *Comput. Phys. Commun.* **191** (2015) 159 [arXiv:1410.3012] [INSPIRE].

[30] P. Skands, S. Carrazza and J. Rojo, *Tuning PYTHIA 8.1: the Monash 2013 Tune*, *Eur. Phys. J. C* **74** (2014) 3024 [arXiv:1404.5630] [INSPIRE].

[31] ALICE collaboration, *The ALICE definition of primary particles*, ALICE-PUBLIC-2017-005 (2017).

[32] ALICE collaboration, *Direct photon production at low transverse momentum in proton-proton collisions at* $\sqrt{s}$ = 2.76 *and* 8 *TeV*, *Phys. Rev. C* **99** (2019) 024912 [arXiv:1803.09857] [INSPIRE].

[33] H. Fritzsch, *Elementary particles: building blocks of matter*, (2005) [DOI:10.1142/5739] [INSPIRE].

[34] ALICE collaboration, *Production of charged pions, kaons, and (anti-)protons in Pb-Pb and inelastic pp collisions at* $\sqrt{s_{NN}}$ = 5.02 *TeV*, *Phys. Rev. C* **101** (2020) 044907 [arXiv:1910.07678] [INSPIRE].

[35] ALICE collaboration, *Transverse momentum spectra and nuclear modification factors of charged particles in pp, p-Pb and Pb-Pb collisions at the LHC*, *JHEP* **11** (2018) 013 [arXiv:1802.09145] [INSPIRE].

[36] S. Roesler, R. Engel and J. Ranft, *The Monte Carlo event generator DPMJET-III*, in the proceedings of the *International Conference on Advanced Monte Carlo for Radiation Physics, Particle Transport Simulation and Applications (MC 2000)*, (2000), p. 1033–1038 [DOI:10.1007/978-3-642-18211-2_166] [hep-ph/0012252] [INSPIRE].

[37] ALICE collaboration, π^0 *and* η *meson production in proton-proton collisions at* $\sqrt{s}$ = 8 *TeV*, *Eur. Phys. J. C* **78** (2018) 263 [arXiv:1708.08745] [INSPIRE].

[38] ALICE collaboration, *Neutral pion and* η *meson production in p-Pb collisions at* $\sqrt{s_{NN}}$ = 5.02 *TeV*, *Eur. Phys. J. C* **78** (2018) 624 [arXiv:1801.07051] [INSPIRE].

[39] ALICE collaboration, *Neutral pion and* η *meson production at mid-rapidity in Pb-Pb collisions at* $\sqrt{s_{NN}}$ = 2.76 *TeV*, *Phys. Rev. C* **98** (2018) 044901 [arXiv:1803.05490] [INSPIRE].

[40] ALICE collaboration, *Production of light-flavor hadrons in pp collisions at* $\sqrt{s}$ = 7 *and* $\sqrt{s}$ = 13 *TeV*, *Eur. Phys. J. C* **81** (2021) 256 [arXiv:2005.11120] [INSPIRE].

[41] ALICE collaboration, *ALICE upgrades during the LHC Long Shutdown 2*, arXiv:2302.01238 [INSPIRE].

[42] ALICE collaboration, *Technical Design Report for the Upgrade of the ALICE Inner Tracking System*, *J. Phys. G* **41** (2014) 087002 [INSPIRE].

2023 JINST 18 P11032

The ALICE collaboration

S. Acharya [125], D. Adamová [86], A. Adler[69], G. Aglieri Rinella [32], M. Agnello [29], N. Agrawal [50], Z. Ahammed [132], S. Ahmad [15], S.U. Ahn [70], I. Ahuja [37], A. Akindinov [140], M. Al-Turany [97], D. Aleksandrov [140], B. Alessandro [55], H.M. Alfanda [6], R. Alfaro Molina [66], B. Ali [15], A. Alici [25], N. Alizadehvandchali [114], A. Alkin [32], J. Alme [20], G. Alocco [51], T. Alt [63], I. Altsybeev [140], M.N. Anaam [6], C. Andrei [45], A. Andronic [135], V. Anguelov[94], F. Antinori [53], P. Antonioli [50], N. Apadula [74], L. Aphecetche [103], H. Appelshäuser [63], C. Arata [73], S. Arcelli [25], M. Aresti [51], R. Arnaldi [55], J.G.M.C.A. Arneiro [110], I.C. Arsene [19], M. Arslandok [137], A. Augustinus [32], R. Averbeck [97], M.D. Azmi [15], A. Badalà [52], J. Bae [104], Y.W. Baek [40], X. Bai [118], R. Bailhache [63], Y. Bailung [47], A. Balbino [29], A. Baldisseri [128], B. Balis [2], D. Banerjee [4], Z. Banoo [91], R. Barbera [26], F. Barile [31], L. Barioglio [95], M. Barlou[78], G.G. Barnaföldi [136], L.S. Barnby [85], V. Barret [125], L. Barreto [110], C. Bartels [117], K. Barth [32], E. Bartsch [63], N. Bastid [125], S. Basu [75], G. Batigne [103], D. Battistini [95], B. Batyunya [141], D. Bauri[46], J.L. Bazo Alba [101], I.G. Bearden [83], C. Beattie [137], P. Becht [97], D. Behera [47], I. Belikov [127], A.D.C. Bell Hechavarria [135], F. Bellini [25], R. Bellwied [114], S. Belokurova [140], G. Bencedi [136], S. Beole [24], A. Bercuci [45], Y. Berdnikov [140], A. Berdnikova [94], L. Bergmann [94], M.G. Besoiu [62], L. Betev [32], P.P. Bhaduri [132], A. Bhasin [91], M.A. Bhat [4], B. Bhattacharjee [41], L. Bianchi [24], N. Bianchi [48], J. Bielčík [35], J. Bielčíková [86], J. Biernat [107], A.P. Bigot [127], A. Bilandzic [95], G. Biro [136], S. Biswas [4], N. Bize [103], J.T. Blair [108], D. Blau [140], M.B. Blidaru [97], N. Bluhme[38], C. Blume [63], G. Boca [21,54], F. Bock [87], T. Bodova [20], A. Bogdanov[140], S. Boi [22], J. Bok [57], L. Boldizsár [136], M. Bombara [37], P.M. Bond [32], G. Bonomi [131,54], H. Borel [128], A. Borissov [140], H. Bossi [137], E. Botta [24], Y.E.M. Bouziani [63], L. Bratrud [63], P. Braun-Munzinger [97], M. Bregant [110], M. Broz [35], G.E. Bruno [96,31], M.D. Buckland [23], D. Budnikov[140], H. Buesching [63], S. Bufalino [29], P. Buhler [102], Z. Buthelezi [67,121], A. Bylinkin [20], S.A. Bysiak[107], M. Cai [6], H. Caines [137], A. Caliva [28], E. Calvo Villar [101], J.M.M. Camacho [109], P. Camerini [23], F.D.M. Canedo [110], M. Carabas [124], A.A. Carballo [32], A.G.B. Carcamo [94], F. Carnesecchi [32], R. Caron [126], L.A.D. Carvalho [110], J. Castillo Castellanos [128], F. Catalano [32,24], C. Ceballos Sanchez [141], I. Chakaberia [74], P. Chakraborty [46], S. Chandra [132], S. Chapeland [32], M. Chartier [117], S. Chattopadhyay [132], S. Chattopadhyay [99], T.G. Chavez [44], T. Cheng [97,6], C. Cheshkov [126], B. Cheynis [126], V. Chibante Barroso [32], D.D. Chinellato [111], E.S. Chizzali [95], J. Cho [57], S. Cho [57], P. Chochula [32], P. Christakoglou [84], C.H. Christensen [83], P. Christiansen [75], T. Chujo [123], M. Ciacco [29], C. Cicalo [51], F. Cindolo [50], M.R. Ciupek[97], G. Clai[II,50], F. Colamaria [49], J.S. Colburn[100], D. Colella [96,31], M. Colocci [25], G. Conesa Balbastre [73], Z. Conesa del Valle [72], G. Contin [23], J.G. Contreras [35], M.L. Coquet [128], T.M. Cormier[I,87], P. Cortese [130,55], M.R. Cosentino [112], F. Costa [32], S. Costanza [21,54], C. Cot [72], J. Crkovská [94], P. Crochet [125], R. Cruz-Torres [74], P. Cui [6], A. Dainese [53], M.C. Danisch [94], A. Danu [62], P. Das [80], P. Das [4], S. Das [4], A.R. Dash [135], S. Dash [46], A. De Caro [28], G. de Cataldo [49], J. de Cuveland[38], A. De Falco [22], D. De Gruttola [28], N. De Marco [55], C. De Martin [23], S. De Pasquale [28], R. Deb[131], S. Deb [47], K.R. Deja[133], R. Del Grande [95], L. Dello Stritto [28], W. Deng [6], P. Dhankher [18], D. Di Bari [31], A. Di Mauro [32],

2023 JINST 18 P11032

B. Diab [128], R.A. Diaz [141,7], T. Dietel [113], Y. Ding [6], R. Divià [32], D.U. Dixit [18], Ø. Djuvsland[20], U. Dmitrieva [140], A. Dobrin [62], B. Dönigus [63], J.M. Dubinski[133], A. Dubla [97], S. Dudi [90], P. Dupieux [125], M. Durkac[106], N. Dzalaiova[12], T.M. Eder [135], R.J. Ehlers [74], F. Eisenhut [63], D. Elia [49], B. Erazmus [103], F. Ercolessi [25], F. Erhardt [89], M.R. Ersdal[20], B. Espagnon [72], G. Eulisse [32], D. Evans [100], S. Evdokimov [140], L. Fabbietti [95], M. Faggin [27], J. Faivre [73], F. Fan [6], W. Fan [74], A. Fantoni [48], M. Fasel [87], P. Fecchio[29], A. Feliciello [55], G. Feofilov [140], A. Fernández Téllez [44], L. Ferrandi [110], M.B. Ferrer [32], A. Ferrero [128], C. Ferrero [55], A. Ferretti [24], V.J.G. Feuillard [94], V. Filova[35], D. Finogeev [140], F.M. Fionda [51], F. Flor [114], A.N. Flores [108], S. Foertsch [67], I. Fokin [94], S. Fokin [140], E. Fragiacomo [56], E. Frajna [136], U. Fuchs [32], N. Funicello [28], C. Furget [73], A. Furs [140], T. Fusayasu [98], J.J. Gaardhøje [83], M. Gagliardi [24], A.M. Gago [101], C.D. Galvan [109], D.R. Gangadharan [114], P. Ganoti [78], C. Garabatos [97], J.R.A. Garcia [44], E. Garcia-Solis [9], C. Gargiulo [32], A. Garibli[81], K. Garner[135], P. Gasik [97], A. Gautam [116], M.B. Gay Ducati [65], M. Germain [103], A. Ghimouz[123], C. Ghosh[132], M. Giacalone [50,25], P. Giubellino [97,55], P. Giubilato [27], A.M.C. Glaenzer [128], P. Glässel [94], E. Glimos[120], D.J.Q. Goh[76], V. Gonzalez [134], S. Gorbunov[38], M. Gorgon [2], K. Goswami [47], S. Gotovac[33], V. Grabski [66], L.K. Graczykowski [133], E. Grecka [86], A. Grelli [58], C. Grigoras [32], V. Grigoriev [140], S. Grigoryan [141,1], F. Grosa [32], J.F. Grosse-Oetringhaus [32], R. Grosso [97], D. Grund [35], G.G. Guardiano [111], R. Guernane [73], M. Guilbaud [103], K. Gulbrandsen [83], T. Gundem [63], T. Gunji [122], W. Guo [6], A. Gupta [91], R. Gupta [91], R. Gupta [47], S.P. Guzman [44], K. Gwizdziel [133], L. Gyulai [136], M.K. Habib[97], C. Hadjidakis [72], F.U. Haider [91], H. Hamagaki [76], A. Hamdi [74], M. Hamid[6], Y. Han [138], B.G. Hanley [134], R. Hannigan [108], J. Hansen [75], M.R. Haque [133], J.W. Harris [137], A. Harton [9], H. Hassan [87], D. Hatzifotiadou [50], P. Hauer [42], L.B. Havener [137], S.T. Heckel [95], E. Hellbär [97], H. Helstrup [34], M. Hemmer [63], T. Herman [35], G. Herrera Corral [8], F. Herrmann[135], S. Herrmann [126], K.F. Hetland [34], B. Heybeck [63], H. Hillemanns [32], B. Hippolyte [127], F.W. Hoffmann [69], B. Hofman [58], B. Hohlweger [84], G.H. Hong [138], M. Horst [95], A. Horzyk [2], Y. Hou [6], P. Hristov [32], C. Hughes [120], P. Huhn[63], L.M. Huhta [115], T.J. Humanic [88], L.A. Husova [135], A. Hutson [114], R. Ilkaev[140], H. Ilyas [13], M. Inaba [123], G.M. Innocenti [32], M. Ippolitov [140], A. Isakov [86], T. Isidori [116], M.S. Islam [99], M. Ivanov [97], M. Ivanov[12], V. Ivanov [140], K.E. Iversen [75], M. Jablonski [2], B. Jacak[74], N. Jacazio [25], P.M. Jacobs [74], S. Jadlovska[106], J. Jadlovsky[106], S. Jaelani [82], C. Jahnke[111], M.J. Jakubowska [133], M.A. Janik [133], T. Janson[69], M. Jercic[89], S. Ji [16], S. Jia [10], A.A.P. Jimenez [64], F. Jonas [87], J.M. Jowett [32,97], J. Jung [63], M. Jung [63], A. Junique [32], A. Jusko [100], M.J. Kabus [32,133], J. Kaewjai[105], P. Kalinak [59], A.S. Kalteyer [97], A. Kalweit [32], V. Kaplin [140], A. Karasu Uysal [71], D. Karatovic [89], O. Karavichev [140], T. Karavicheva [140], P. Karczmarczyk [133], E. Karpechev [140], U. Kebschull [69], R. Keidel [139], D.L.D. Keijdener[58], M. Keil [32], B. Ketzer [42], S.S. Khade [47], A.M. Khan [6], S. Khan [15], A. Khanzadeev [140], Y. Kharlov [140], A. Khatun [116], A. Khuntia [107], M.B. Kidson[113], B. Kileng [34], B. Kim [104], C. Kim [16], D.J. Kim [115], E.J. Kim [68], J. Kim [138], J.S. Kim [40], J. Kim [57], J. Kim [68], M. Kim [18], S. Kim [17], T. Kim [138], K. Kimura [92], S. Kirsch [63], I. Kisel [38], S. Kiselev [140], A. Kisiel [133], J.P. Kitowski [2], J.L. Klay [5], J. Klein [32], S. Klein [74], C. Klein-Bösing [135], M. Kleiner [63], T. Klemenz [95], A. Kluge [32], A.G. Knospe [114], C. Kobdaj [105], T. Kollegger[97], A. Kondratyev [141], N. Kondratyeva [140], E. Kondratyuk [140], J. Konig [63], S.A. Konigstorfer [95], P.J. Konopka [32], G. Kornakov [133],

2023 JINST 18 P11032

S.D. Koryciak [2], A. Kotliarov [86], V. Kovalenko [140], M. Kowalski [107], V. Kozhuharov [36], I. Králik [59], A. Kravčáková [37], L. Krcal [32,38], M. Krivda [100,59], F. Krizek [86], K. Krizkova Gajdosova [32], M. Kroesen [94], M. Krüger [63], D.M. Krupova [35], E. Kryshen [140], V. Kučera [57], C. Kuhn [127], P.G. Kuijer [84], T. Kumaoka[123], D. Kumar[132], L. Kumar [90], N. Kumar[90], S. Kumar [31], S. Kundu [32], P. Kurashvili [79], A. Kurepin [140], A.B. Kurepin [140], A. Kuryakin [140], S. Kushpil [86], J. Kvapil [100], M.J. Kweon [57], Y. Kwon [138], S.L. La Pointe [38], P. La Rocca [26], A. Lakrathok[105], M. Lamanna [32], R. Langoy [119], P. Larionov [32], E. Laudi [32], L. Lautner [32,95], R. Lavicka [102], R. Lea [131,54], L. Leardini[94], H. Lee [104], I. Legrand [45], G. Legras [135], J. Lehrbach [38], T.M. Lelek[2], R.C. Lemmon [85], I. León Monzón [109], M.M. Lesch [95], E.D. Lesser [18], P. Lévai [136], X. Li[10], X.L. Li[6], J. Lien [119], R. Lietava [100], I. Likmeta [114], B. Lim [24], S.H. Lim [16], V. Lindenstruth [38], A. Lindner[45], C. Lippmann [97], A. Liu [18], D.H. Liu [6], J. Liu [117], G.S.S. Liveraro [111], I.M. Lofnes [20], C. Loizides [87], S. Lokos [107], J. Lomker [58], P. Loncar [33], J.A. Lopez [94], X. Lopez [125], E. López Torres [7], P. Lu [97,118], J.R. Luhder [135], M. Lunardon [27], G. Luparello [56], Y.G. Ma [39], M. Mager [32], A. Maire [127], M.V. Makariev [36], M. Malaev [140], G. Malfattore [25], N.M. Malik [91], Q.W. Malik[19], S.K. Malik [91], L. Malinina [V,141], D. Mallick [80], N. Mallick [47], G. Mandaglio [30,52], S.K. Mandal [79], V. Manko [140], F. Manso [125], V. Manzari [49], Y. Mao [6], R.W. Marcjan [2], G.V. Margagliotti [23], A. Margotti [50], A. Marín [97], C. Markert [108], P. Martinengo [32], M.I. Martínez [44], G. Martínez García [103], M.P.P. Martins [110], S. Masciocchi [97], M. Masera [24], A. Masoni [51], L. Massacrier [72], A. Mastroserio [129,49], O. Matonoha [75], S. Mattiazzo [27], P.F.T. Matuoka[110], A. Matyja [107], C. Mayer [107], A.L. Mazuecos [32], F. Mazzaschi [24], M. Mazzilli [32], J.E. Mdhluli [121], A.F. Mechler[63], Y. Melikyan [43,140], A. Menchaca-Rocha [66], E. Meninno [102,28], A.S. Menon [114], M. Meres [12], S. Mhlanga[113,67], Y. Miake[123], L. Micheletti [32], L.C. Migliorin[126], D.L. Mihaylov [95], K. Mikhaylov [141,140], A.N. Mishra [136], D. Miśkowiec [97], A. Modak [4], A.P. Mohanty [58], B. Mohanty [80], M. Mohisin Khan [III,15], M.A. Molander [43], Z. Moravcova [83], C. Mordasini [95], D.A. Moreira De Godoy [135], I. Morozov [140], A. Morsch [32], T. Mrnjavac [32], V. Muccifora [48], S. Muhuri [132], J.D. Mulligan [74], A. Mulliri[22], M.G. Munhoz [110], R.H. Munzer [63], H. Murakami [122], S. Murray [113], L. Musa [32], J. Musinsky [59], J.W. Myrcha [133], B. Naik [121], A.I. Nambrath [18], B.K. Nandi[46], R. Nania [50], E. Nappi [49], A.F. Nassirpour [17,75], A. Nath [94], C. Nattrass [120], M.N. Naydenov [36], A. Neagu[19], A. Negru[124], L. Nellen [64], G. Neskovic [38], B.S. Nielsen [83], E.G. Nielsen [83], S. Nikolaev [140], S. Nikulin [140], V. Nikulin [140], F. Noferini [50], S. Noh [11], P. Nomokonov [141], J. Norman [117], N. Novitzky [123], P. Nowakowski [133], A. Nyanin [140], J. Nystrand [20], M. Ogino [76], A. Ohlson [75], V.A. Okorokov [140], J. Oleniacz [133], A.C. Oliveira Da Silva [120], M.H. Oliver [137], A. Onnerstad [115], C. Oppedisano [55], A. Ortiz Velasquez [64], J. Otwinowski [107], M. Oya[92], K. Oyama [76], Y. Pachmayer [94], S. Padhan [46], D. Pagano [131,54], G. Paić [64], A. Palasciano [49], S. Panebianco [128], H. Park [123], H. Park [104], J. Park [57], J.E. Parkkila [32], R.N. Patra[91], B. Paul [22], H. Pei [6], T. Peitzmann [58], X. Peng [6], M. Pennisi [24], D. Peresunko [140], G.M. Perez [7], S. Perrin [128], Y. Pestov[140], V. Petrov [140], M. Petrovici [45], R.P. Pezzi [103,65], S. Piano [56], M. Pikna [12], P. Pillot [103], O. Pinazza [50,32], L. Pinsky[114], C. Pinto [95], S. Pisano [48], M. Płoskoń [74], M. Planinic[89], F. Pliquett[63], M.G. Poghosyan [87], B. Polichtchouk [140], S. Politano [29], N. Poljak [89], A. Pop [45], S. Porteboeuf-Houssais [125], V. Pozdniakov [141],

2023 JINST 18 P11032

I.Y. Pozos [44], K.K. Pradhan [47], S.K. Prasad [4], S. Prasad [47], R. Preghenella [50], F. Prino [55], C.A. Pruneau [134], I. Pshenichnov [140], M. Puccio [32], S. Pucillo [24], Z. Pugelova[106], S. Qiu [84], L. Quaglia [24], R.E. Quishpe[114], S. Ragoni [14], A. Rakotozafindrabe [128], L. Ramello [130,55], F. Rami [127], S.A.R. Ramirez [44], T.A. Rancien[73], M. Rasa [26], S.S. Räsänen [43], R. Rath [50], M.P. Rauch [20], I. Ravasenga [84], K.F. Read [87,120], C. Reckziegel [112], A.R. Redelbach [38], K. Redlich [IV,79], C.A. Reetz [97], A. Rehman[20], F. Reidt [32], H.A. Reme-Ness [34], Z. Rescakova[37], K. Reygers [94], A. Riabov [140], V. Riabov [140], R. Ricci [28], M. Richter[19], A.A. Riedel [95], W. Riegler [32], C. Ristea [62], M.V. Rodriguez [32], M. Rodríguez Cahuantzi [44], K. Røed [19], R. Rogalev [140], E. Rogochaya [141], T.S. Rogoschinski [63], D. Rohr [32], D. Röhrich [20], P.F. Rojas[44], S. Rojas Torres [35], P.S. Rokita [133], G. Romanenko [141], F. Ronchetti [48], A. Rosano [30,52], E.D. Rosas[64], K. Roslon [133], A. Rossi [53], A. Roy [47], S. Roy[46], N. Rubini [25], O.V. Rueda [114], D. Ruggiano [133], R. Rui [23], P.G. Russek [2], R. Russo [84], A. Rustamov [81], E. Ryabinkin [140], Y. Ryabov [140], A. Rybicki [107], H. Rytkonen [115], J. Ryu [16], W. Rzesa [133], O.A.M. Saarimaki [43], R. Sadek [103], S. Sadhu [31], S. Sadovsky [140], J. Saetre [20], K. Šafařík [35], P. Saha[41], S.K. Saha [4], S. Saha [80], B. Sahoo [46], B. Sahoo [47], R. Sahoo [47], S. Sahoo[60], D. Sahu [47], P.K. Sahu [60], J. Saini [132], K. Sajdakova[37], S. Sakai [123], M.P. Salvan [97], S. Sambyal [91], I. Sanna [32,95], T.B. Saramela[110], D. Sarkar [134], N. Sarkar[132], P. Sarma[41], V. Sarritzu [22], V.M. Sarti [95], M.H.P. Sas [137], J. Schambach [87], H.S. Scheid [63], C. Schiaua [45], R. Schicker [94], A. Schmah[94], C. Schmidt [97], H.R. Schmidt[93], M.O. Schmidt [32], M. Schmidt[93], N.V. Schmidt [87], A.R. Schmier [120], R. Schotter [127], A. Schröter [38], J. Schukraft [32], K. Schwarz[97], K. Schweda [97], G. Scioli [25], E. Scomparin [55], J.E. Seger [14], Y. Sekiguchi[122], D. Sekihata [122], I. Selyuzhenkov [97], S. Senyukov [127], J.J. Seo [57], D. Serebryakov [140], L. Šerkšnytė [95], A. Sevcenco [62], T.J. Shaba [67], A. Shabetai [103], R. Shahoyan[32], A. Shangaraev [140], A. Sharma[90], B. Sharma [91], D. Sharma [46], H. Sharma [53,107], M. Sharma [91], S. Sharma [76], S. Sharma [91], U. Sharma [91], A. Shatat [72], O. Sheibani[114], K. Shigaki [92], M. Shimomura[77], J. Shin[11], S. Shirinkin [140], Q. Shou [39], Y. Sibiriak [140], S. Siddhanta [51], T. Siemiarczuk [79], T.F. Silva [110], D. Silvermyr [75], T. Simantathammakul[105], R. Simeonov [36], B. Singh[91], B. Singh [95], K. Singh [47], R. Singh [80], R. Singh [91], R. Singh [47], S. Singh [15], V.K. Singh [132], V. Singhal [132], T. Sinha [99], B. Sitar [12], M. Sitta [130,55], T.B. Skaali[19], G. Skorodumovs [94], M. Slupecki [43], N. Smirnov [137], R.J.M. Snellings [58], E.H. Solheim [19], J. Song [114], A. Songmoolnak[105], C. Sonnabend [32,97], F. Soramel [27], A.B. Soto-hernandez[88], R. Spijkers [84], I. Sputowska [107], J. Staa [75], J. Stachel [94], I. Stan [62], P.J. Steffanic [120], S.F. Stiefelmaier [94], D. Stocco [103], I. Storehaug [19], P. Stratmann [135], S. Strazzi [25], C.P. Stylianidis[84], A.A.P. Suaide [110], C. Suire [72], M. Sukhanov [140], M. Suljic [32], R. Sultanov [140], V. Sumberia [91], S. Sumowidagdo [82], S. Swain[60], I. Szarka [12], M. Szymkowski[133], S.F. Taghavi [95], G. Taillepied [97], J. Takahashi [111], G.J. Tambave [80], S. Tang [6], Z. Tang [118], J.D. Tapia Takaki [116], N. Tapus[124], M.G. Tarzila[45], G.F. Tassielli [31], A. Tauro [32], G. Tejeda Muñoz [44], A. Telesca [32], L. Terlizzi [24], C. Terrevoli [114], S. Thakur [4], D. Thomas [108], A. Tikhonov [140], A.R. Timmins [114], M. Tkacik[106], T. Tkacik [106], A. Toia [63], R. Tokumoto[92], N. Topilskaya [140], M. Toppi [48], T. Tork [72], A.G. Torres Ramos [31], A. Trifiró [30,52], A.S. Triolo [32,30,52], S. Tripathy [50], T. Tripathy [46], S. Trogolo [32], V. Trubnikov [3], W.H. Trzaska [115], T.P. Trzcinski [133], A. Tumkin[140], R. Turrisi [53], T.S. Tveter [19], K. Ullaland [20], B. Ulukutlu [95], A. Uras [126], M. Urioni [54,131], G.L. Usai [22], M. Vala[37], N. Valle [21], L.V.R. van

2023 JINST 18 P11032

Doremalen[58], M. van Leeuwen [84], C.A. van Veen [94], R.J.G. van Weelden [84], P. Vande Vyvre [32], D. Varga [136], Z. Varga [136], M. Vasileiou [78], A. Vasiliev [140], O. Vázquez Doce [48], V. Vechernin [140], E. Vercellin [24], S. Vergara Limón[44], L. Vermunt [97], R. Vértesi [136], M. Verweij [58], L. Vickovic[33], Z. Vilakazi[121], O. Villalobos Baillie [100], A. Villani [23], G. Vino [49], A. Vinogradov [140], T. Virgili [28], M.M.O. Virta [115], V. Vislavicius[75], A. Vodopyanov [141], B. Volkel [32], M.A. Völkl [94], K. Voloshin[140], S.A. Voloshin [134], G. Volpe [31], B. von Haller [32], I. Vorobyev [95], N. Vozniuk [140], J. Vrláková [37], J. Wan[39], C. Wang [39], D. Wang[39], Y. Wang [39], A. Wegrzynek [32], F.T. Weiglhofer[38], S.C. Wenzel [32], J.P. Wessels [135], S.L. Weyhmiller [137], J. Wiechula [63], J. Wikne [19], G. Wilk [79], J. Wilkinson [97], G.A. Willems [135], B. Windelband[94], M. Winn [128], J.R. Wright [108], W. Wu[39], Y. Wu [118], R. Xu [6], A. Yadav [42], A.K. Yadav [132], S. Yalcin [71], Y. Yamaguchi[92], S. Yang[20], S. Yano [92], Z. Yin [6], I.-K. Yoo [16], J.H. Yoon [57], H. Yu[11], S. Yuan[20], A. Yuncu [94], V. Zaccolo [23], C. Zampolli [32], F. Zanone [94], N. Zardoshti [32], A. Zarochentsev [140], P. Závada [61], N. Zaviyalov[140], M. Zhalov [140], B. Zhang [6], L. Zhang [39], S. Zhang [39], X. Zhang [6], Y. Zhang[118], Z. Zhang [6], M. Zhao [10], V. Zherebchevskii [140], Y. Zhi[10], D. Zhou [6], Y. Zhou [83], J. Zhu [97,6], Y. Zhu[6], S.C. Zugravel [55], N. Zurlo [131,54]

[1] *A.I. Alikhanyan National Science Laboratory (Yerevan Physics Institute) Foundation, Yerevan, Armenia*
[2] *AGH University of Science and Technology, Cracow, Poland*
[3] *Bogolyubov Institute for Theoretical Physics, National Academy of Sciences of Ukraine, Kiev, Ukraine*
[4] *Bose Institute, Department of Physics and Centre for Astroparticle Physics and Space Science (CAPSS), Kolkata, India*
[5] *California Polytechnic State University, San Luis Obispo, California, United States*
[6] *Central China Normal University, Wuhan, China*
[7] *Centro de Aplicaciones Tecnológicas y Desarrollo Nuclear (CEADEN), Havana, Cuba*
[8] *Centro de Investigación y de Estudios Avanzados (CINVESTAV), Mexico City and Mérida, Mexico*
[9] *Chicago State University, Chicago, Illinois, United States*
[10] *China Institute of Atomic Energy, Beijing, China*
[11] *Chungbuk National University, Cheongju, Republic of Korea*
[12] *Comenius University Bratislava, Faculty of Mathematics, Physics and Informatics, Bratislava, Slovak Republic*
[13] *COMSATS University Islamabad, Islamabad, Pakistan*
[14] *Creighton University, Omaha, Nebraska, United States*
[15] *Department of Physics, Aligarh Muslim University, Aligarh, India*
[16] *Department of Physics, Pusan National University, Pusan, Republic of Korea*
[17] *Department of Physics, Sejong University, Seoul, Republic of Korea*
[18] *Department of Physics, University of California, Berkeley, California, United States*
[19] *Department of Physics, University of Oslo, Oslo, Norway*
[20] *Department of Physics and Technology, University of Bergen, Bergen, Norway*
[21] *Dipartimento di Fisica, Università di Pavia, Pavia, Italy*
[22] *Dipartimento di Fisica dell'Università and Sezione INFN, Cagliari, Italy*
[23] *Dipartimento di Fisica dell'Università and Sezione INFN, Trieste, Italy*
[24] *Dipartimento di Fisica dell'Università and Sezione INFN, Turin, Italy*
[25] *Dipartimento di Fisica e Astronomia dell'Università and Sezione INFN, Bologna, Italy*
[26] *Dipartimento di Fisica e Astronomia dell'Università and Sezione INFN, Catania, Italy*
[27] *Dipartimento di Fisica e Astronomia dell'Università and Sezione INFN, Padova, Italy*
[28] *Dipartimento di Fisica 'E.R. Caianiello' dell'Università and Gruppo Collegato INFN, Salerno, Italy*
[29] *Dipartimento DISAT del Politecnico and Sezione INFN, Turin, Italy*
[30] *Dipartimento di Scienze MIFT, Università di Messina, Messina, Italy*
[31] *Dipartimento Interateneo di Fisica 'M. Merlin' and Sezione INFN, Bari, Italy*
[32] *European Organization for Nuclear Research (CERN), Geneva, Switzerland*

2023 JINST 18 P11032

[33] *Faculty of Electrical Engineering, Mechanical Engineering and Naval Architecture, University of Split, Split, Croatia*
[34] *Faculty of Engineering and Science, Western Norway University of Applied Sciences, Bergen, Norway*
[35] *Faculty of Nuclear Sciences and Physical Engineering, Czech Technical University in Prague, Prague, Czech Republic*
[36] *Faculty of Physics, Sofia University, Sofia, Bulgaria*
[37] *Faculty of Science, P.J. Šafárik University, Košice, Slovak Republic*
[38] *Frankfurt Institute for Advanced Studies, Johann Wolfgang Goethe-Universität Frankfurt, Frankfurt, Germany*
[39] *Fudan University, Shanghai, China*
[40] *Gangneung-Wonju National University, Gangneung, Republic of Korea*
[41] *Gauhati University, Department of Physics, Guwahati, India*
[42] *Helmholtz-Institut für Strahlen- und Kernphysik, Rheinische Friedrich-Wilhelms-Universität Bonn, Bonn, Germany*
[43] *Helsinki Institute of Physics (HIP), Helsinki, Finland*
[44] *High Energy Physics Group, Universidad Autónoma de Puebla, Puebla, Mexico*
[45] *Horia Hulubei National Institute of Physics and Nuclear Engineering, Bucharest, Romania*
[46] *Indian Institute of Technology Bombay (IIT), Mumbai, India*
[47] *Indian Institute of Technology Indore, Indore, India*
[48] *INFN, Laboratori Nazionali di Frascati, Frascati, Italy*
[49] *INFN, Sezione di Bari, Bari, Italy*
[50] *INFN, Sezione di Bologna, Bologna, Italy*
[51] *INFN, Sezione di Cagliari, Cagliari, Italy*
[52] *INFN, Sezione di Catania, Catania, Italy*
[53] *INFN, Sezione di Padova, Padova, Italy*
[54] *INFN, Sezione di Pavia, Pavia, Italy*
[55] *INFN, Sezione di Torino, Turin, Italy*
[56] *INFN, Sezione di Trieste, Trieste, Italy*
[57] *Inha University, Incheon, Republic of Korea*
[58] *Institute for Gravitational and Subatomic Physics (GRASP), Utrecht University/Nikhef, Utrecht, Netherlands*
[59] *Institute of Experimental Physics, Slovak Academy of Sciences, Košice, Slovak Republic*
[60] *Institute of Physics, Homi Bhabha National Institute, Bhubaneswar, India*
[61] *Institute of Physics of the Czech Academy of Sciences, Prague, Czech Republic*
[62] *Institute of Space Science (ISS), Bucharest, Romania*
[63] *Institut für Kernphysik, Johann Wolfgang Goethe-Universität Frankfurt, Frankfurt, Germany*
[64] *Instituto de Ciencias Nucleares, Universidad Nacional Autónoma de México, Mexico City, Mexico*
[65] *Instituto de Física, Universidade Federal do Rio Grande do Sul (UFRGS), Porto Alegre, Brazil*
[66] *Instituto de Física, Universidad Nacional Autónoma de México, Mexico City, Mexico*
[67] *iThemba LABS, National Research Foundation, Somerset West, South Africa*
[68] *Jeonbuk National University, Jeonju, Republic of Korea*
[69] *Johann-Wolfgang-Goethe Universität Frankfurt Institut für Informatik, Fachbereich Informatik und Mathematik, Frankfurt, Germany*
[70] *Korea Institute of Science and Technology Information, Daejeon, Republic of Korea*
[71] *KTO Karatay University, Konya, Turkey*
[72] *Laboratoire de Physique des 2 Infinis, Irène Joliot-Curie, Orsay, France*
[73] *Laboratoire de Physique Subatomique et de Cosmologie, Université Grenoble-Alpes, CNRS-IN2P3, Grenoble, France*
[74] *Lawrence Berkeley National Laboratory, Berkeley, California, United States*
[75] *Lund University Department of Physics, Division of Particle Physics, Lund, Sweden*
[76] *Nagasaki Institute of Applied Science, Nagasaki, Japan*
[77] *Nara Women's University (NWU), Nara, Japan*
[78] *National and Kapodistrian University of Athens, School of Science, Department of Physics , Athens, Greece*
[79] *National Centre for Nuclear Research, Warsaw, Poland*
[80] *National Institute of Science Education and Research, Homi Bhabha National Institute, Jatni, India*

2023 JINST 18 P11032

[81] *National Nuclear Research Center, Baku, Azerbaijan*
[82] *National Research and Innovation Agency - BRIN, Jakarta, Indonesia*
[83] *Niels Bohr Institute, University of Copenhagen, Copenhagen, Denmark*
[84] *Nikhef, National institute for subatomic physics, Amsterdam, Netherlands*
[85] *Nuclear Physics Group, STFC Daresbury Laboratory, Daresbury, United Kingdom*
[86] *Nuclear Physics Institute of the Czech Academy of Sciences, Husinec-Řež, Czech Republic*
[87] *Oak Ridge National Laboratory, Oak Ridge, Tennessee, United States*
[88] *Ohio State University, Columbus, Ohio, United States*
[89] *Physics department, Faculty of science, University of Zagreb, Zagreb, Croatia*
[90] *Physics Department, Panjab University, Chandigarh, India*
[91] *Physics Department, University of Jammu, Jammu, India*
[92] *Physics Program and International Institute for Sustainability with Knotted Chiral Meta Matter (SKCM2), Hiroshima University, Hiroshima, Japan*
[93] *Physikalisches Institut, Eberhard-Karls-Universität Tübingen, Tübingen, Germany*
[94] *Physikalisches Institut, Ruprecht-Karls-Universität Heidelberg, Heidelberg, Germany*
[95] *Physik Department, Technische Universität München, Munich, Germany*
[96] *Politecnico di Bari and Sezione INFN, Bari, Italy*
[97] *Research Division and ExtreMe Matter Institute EMMI, GSI Helmholtzzentrum für Schwerionenforschung GmbH, Darmstadt, Germany*
[98] *Saga University, Saga, Japan*
[99] *Saha Institute of Nuclear Physics, Homi Bhabha National Institute, Kolkata, India*
[100] *School of Physics and Astronomy, University of Birmingham, Birmingham, United Kingdom*
[101] *Sección Física, Departamento de Ciencias, Pontificia Universidad Católica del Perú, Lima, Peru*
[102] *Stefan Meyer Institut für Subatomare Physik (SMI), Vienna, Austria*
[103] *SUBATECH, IMT Atlantique, Nantes Université, CNRS-IN2P3, Nantes, France*
[104] *Sungkyunkwan University, Suwon City, Republic of Korea*
[105] *Suranaree University of Technology, Nakhon Ratchasima, Thailand*
[106] *Technical University of Košice, Košice, Slovak Republic*
[107] *The Henryk Niewodniczanski Institute of Nuclear Physics, Polish Academy of Sciences, Cracow, Poland*
[108] *The University of Texas at Austin, Austin, Texas, United States*
[109] *Universidad Autónoma de Sinaloa, Culiacán, Mexico*
[110] *Universidade de São Paulo (USP), São Paulo, Brazil*
[111] *Universidade Estadual de Campinas (UNICAMP), Campinas, Brazil*
[112] *Universidade Federal do ABC, Santo Andre, Brazil*
[113] *University of Cape Town, Cape Town, South Africa*
[114] *University of Houston, Houston, Texas, United States*
[115] *University of Jyväskylä, Jyväskylä, Finland*
[116] *University of Kansas, Lawrence, Kansas, United States*
[117] *University of Liverpool, Liverpool, United Kingdom*
[118] *University of Science and Technology of China, Hefei, China*
[119] *University of South-Eastern Norway, Kongsberg, Norway*
[120] *University of Tennessee, Knoxville, Tennessee, United States*
[121] *University of the Witwatersrand, Johannesburg, South Africa*
[122] *University of Tokyo, Tokyo, Japan*
[123] *University of Tsukuba, Tsukuba, Japan*
[124] *University Politehnica of Bucharest, Bucharest, Romania*
[125] *Université Clermont Auvergne, CNRS/IN2P3, LPC, Clermont-Ferrand, France*
[126] *Université de Lyon, CNRS/IN2P3, Institut de Physique des 2 Infinis de Lyon, Lyon, France*
[127] *Université de Strasbourg, CNRS, IPHC UMR 7178, F-67000 Strasbourg, France, Strasbourg, France*
[128] *Université Paris-Saclay Centre d'Etudes de Saclay (CEA), IRFU, Département de Physique Nucléaire (DPhN), Saclay, France*
[129] *Università degli Studi di Foggia, Foggia, Italy*

2023 JINST 18 P11032

[130] *Università del Piemonte Orientale, Vercelli, Italy*
[131] *Università di Brescia, Brescia, Italy*
[132] *Variable Energy Cyclotron Centre, Homi Bhabha National Institute, Kolkata, India*
[133] *Warsaw University of Technology, Warsaw, Poland*
[134] *Wayne State University, Detroit, Michigan, United States*
[135] *Westfälische Wilhelms-Universität Münster, Institut für Kernphysik, Münster, Germany*
[136] *Wigner Research Centre for Physics, Budapest, Hungary*
[137] *Yale University, New Haven, Connecticut, United States*
[138] *Yonsei University, Seoul, Republic of Korea*
[139] *Zentrum für Technologie und Transfer (ZTT), Worms, Germany*
[140] *Affiliated with an institute covered by a cooperation agreement with CERN*
[141] *Affiliated with an international laboratory covered by a cooperation agreement with CERN*

[I] *Deceased*
[II] *Also at: Italian National Agency for New Technologies, Energy and Sustainable Economic Development (ENEA), Bologna, Italy*
[III] *Also at: Department of Applied Physics, Aligarh Muslim University, Aligarh, India*
[IV] *Also at: Institute of Theoretical Physics, University of Wroclaw, Poland*
[V] *Also at: An institution covered by a cooperation agreement with CERN*

2023 JINST 18 P11032